J Solid State Electrochem (2012) 16:739–745
DOI 10.1007/s10008-011-1420-x

ORIGINAL PAPER

# Direct electrochemistry of glucose oxidase immobilized on porous carbon nanofiber/room temperature ionic liquid/chitosan composite film and its biosensing application

**Qinglin Sheng · Ruixiao Liu · Jianbin Zheng · Wanghua Lin · Yuanyao Li**

Received: 19 December 2010 / Revised: 19 April 2011 / Accepted: 26 April 2011 / Published online: 12 May 2011


**Abstract** The direct electron transfer of glucose oxidase (GOD) immobilized on a composite matrix based on porous carbon nanofibers (PCNFs), room-temperature ionic liquid (RTIL), and chitosan (CHIT) underlying on a glassy carbon electrode was achieved. The combination of the PCNFs, RTIL, and CHIT provided a suitable microenvironment for GOD to transfer electron directly. In deaerated buffer solutions (pH 7.0), the cyclic voltammetry of the GOD/PCNFs/RTIL/CHIT composite films showed a pair of well-defined redox peaks with the formal potential of −0.45 V (vs. SCE). The synergistic effort of the PCNFs, RTIL, and CHIT also promoted the stability of GOD in the composite film and retained its bioactivity.

**Keywords** Porous carbon nanofiber · Room-temperature ionic liquid · Glucose oxidase · Direct electrochemistry · Biosensor

## Introduction

In recent years, direct electrochemistry of biologically important proteins has been extensively studied due to its significance in both theoretical and practical applications [1–4]. These studies provide the insight into physiological electron transfer processes as well as the designing of label-free biosensors, biofuel cells, and studies of structures and mechanisms of different enzymatic reactions in biological systems [5].

Glucose oxidase (GOD), containing a flavin adenine dinucleotide (FAD) redox center that catalyzes the electron transfer from glucose to gluconolactone, has been extensively used to monitor the glucose levels in diabetics. However, direct electron transfer between GOD and electrode cannot be achieved easily, since FAD, the active site of GOD, is deeply embedded within a protective protein shell. Thus, various nanomaterials or nanocomposites have been used to promote the electron transfer of redox proteins [2–10]. Shan et al. reported the direct electron transfer between GOD and the underlying glassy carbon electrode (GCE) can be readily achieved via colloidal laponite nanoparticles as immobilization matrix [11]. Zhang et al. have synthesized a novel polymeric ionic liquid/graphene nanocomposite for GOD immobilization and the direct electron transfer between GOD and the GC electrode was realized [12]. Recently, Wang et al. reported the integration of graphene–CdS composites with GOD and a glucose biosensor was fabricated [13]. They found that the graphene–CdS nanocomposite exhibited excellent electron transfer properties for GOD due to the synergy effect of graphene sheet and CdS nanocrystals provide a potent strategy to enhance biosensor performance due to their unique physicochemical properties. Heller's group has investigated the wiring of GOD and their application in glucose detection [14–16]. For example, they reported the incorporation of GOD in the hydrogel (by cross-linking acid-templated polyaniline with poly(ethylene glycol) diglycidyl ether) led to electrical wiring of the enzyme and formation of a glucose electrooxidation catalyst [16]. Willner's group have reported the reconstitution of GOD

Q. Sheng · R. Liu · J. Zheng (✉)
Institute of Analytical Science/Shaanxi Provincial Key Laboratory of Electroanalytical Chemistry, Northwest University, Xi'an, Shaanxi 710069, China
e-mail: zhengjb@nwu.edu.cn

W. Lin · Y. Li
Department of Chemical Engineering, National Chung Cheng University, Chia-Yi 62102 Taiwan, Republic of China

and the use of nanoparticles which enabled excellent wiring of the enzyme to the electrode [17, 18]. Among various nanomaterials, carbon nanomaterials have attracted considerable attention for the construction of biosensors due to their good electrical conductivity, unique structural and catalytic properties, good stability, and excellent penetrability [19, 20]. Among them, carbon nanofibers (CNFs) are extremely attractive in bioanalytical area as they can combine properties of high surface area, non-toxicity, and acceptable biocompatibility [21–23]. More recently, Li et al. reported the construction of mediator-free hemoglobin-based $H_2O_2$ biosensor [22]. Ju et al. reported the application of soluble CNF for biosensing of glucose [24], dihydronicotinamide adenine dinucleotide and ethanol [25], and K562 cells [26].

Room-temperature ionic liquids (RTILs) are ionic media resulting from the combination of organic cations and various anions. They have good ionic conductivity, non-volatility, high thermal stability, and viscosity [27, 28]. Recently, one of the most exciting developments is the application of RTILs-related composites for biomolecular immobilization, biocatalysis and the direct electrochemistry of redox proteins. Li et al. studied the influence of RTILs on the direct electrochemistry of GOD entrapped in nanogold-*N*,*N*-dimethylformamide composite film [29]. Liu et al. reported the immobilization of Laccase on the CNTs–RTIL gel film-modified electrode and the combination of CNTs with RTIL showed an improved stability [30]. Zhang et al. reported the fabrication of a CNTs/GOD bionanocomposite bridged by IL-like unit [31]. Therefore, it is believed that the combination of RTILs with novel nanomaterials provide an alternative method to easily immobilize biomolecules so as to prepare enzyme-based biosensors. Porous CNFs (PCNFs), a different morphology from that of conventional CNFs, were suggested to be a good nanomaterial for protein immobilization due to the large surface area and high pore nanostructures.

In this work, the direct electrochemistry of GOD immobilized on a composite film which consists of PCNFs, 1-butyl-3-methylimidazolium hexafluorophosphate (BMIM·$PF_6$), and chitosan (CHIT) was described and characterized. The reduction of $O_2$ is catalyzed, thus the determination of glucose can be achieved. It is expected that the proposed protocol holds great promise for the construction of reagentless enzyme-based biosensors.

## Experimental

### Materials and chemicals

PCNFs shown in Fig. 1 (scanning electron microscopy (SEM) and transmission electron microscopy (TEM) images) with rough surfaces and highly porous structures with 40–60 nm in diameter and several micrometers in length were synthesized and characterized from our previous work [32]. BMIM·$PF_6$ was synthesized and purified according to a previous report [33]. GOD (E.C. 1.1.3.4, 182 U $mg^{-1}$, Type X-S from *Aspergillus niger*), *β-D*(+)-glucose, *o*-dianisidine, and peroxidase were purchased from Sigma and used without further purification. CHIT (MW $1\times10^6$, >90% deacetylation) was from Shanghai Reagent Company (China). All solutions were prepared with ultrapure water (>18 MΩ cm) obtained from a Millipore Milli-Q water purification system.

### Apparatus

An electrochemistry workstation (CHI660A Shanghai Chenhua Instruments Co. Ltd., China) was employed for all the electrochemical measurements. A three-electrode system, where a standard saturated calomel electrode (SCE) served as reference electrode, a platinum wire electrode as the auxiliary electrode, and the prepared electrodes as the working electrode. UV–vis spectra of the prepared composite films were recorded by a Shimadzu UV-2501PC spectrophotometer on an ITO glass, which was cleaned in an ultrasonic bath with acetone, ethanol, and rinsed in deionized water. After drying, the ITO glass was used to prepare composite films similar to that on GCE as described in the following section. Scanning electron microscopic measurements were carried out on a scanning electron microscope (JEOL JSM-6700 F) at 15 kV. The morphology of PCNFs was characterized by transmission electron microscopy (JEM-1230, HITACHI, Japan) operating at 80 kV. The atomic force microscope (AFM) was a digital Instruments Multimode SPM-9500J3 (Shimadzu Corporation, Japan), operating in ex situ Tapping Model.

### Preparation of electrodes

A GCE (3 mm diameter) was firstly polished by a polishing cloth with successively smaller particles of alumina (0.05 μm diameter), rinsed with water, and then ultrasonicated in ethanol and ultrapure water. The enzyme electrode was prepared by a casting method. Typically, appropriate amount of GOD, 50 μL pure BMIM·$PF_6$ and 2 mg PCNFs were added into 1.0 mL CHIT solution, then ultrasonicated for 15 min to form a homogenous solution. Six microliters of the above solution was cast onto the surface of the GCE by using a syringe to prepare the GOD/PCNFs/BMIM·$PF_6$/CHIT/GCEs. The dried GOD/BMIM·$PF_6$/CHIT/GCEs were stored at 4 °C before use. Such a procedure yielded robust GOD/PCNFs/BMIM·$PF_6$/CHIT/GCEs surface films with an average thickness of 2.0±0.1 μm in a dry state (observed by SEM of the vertical

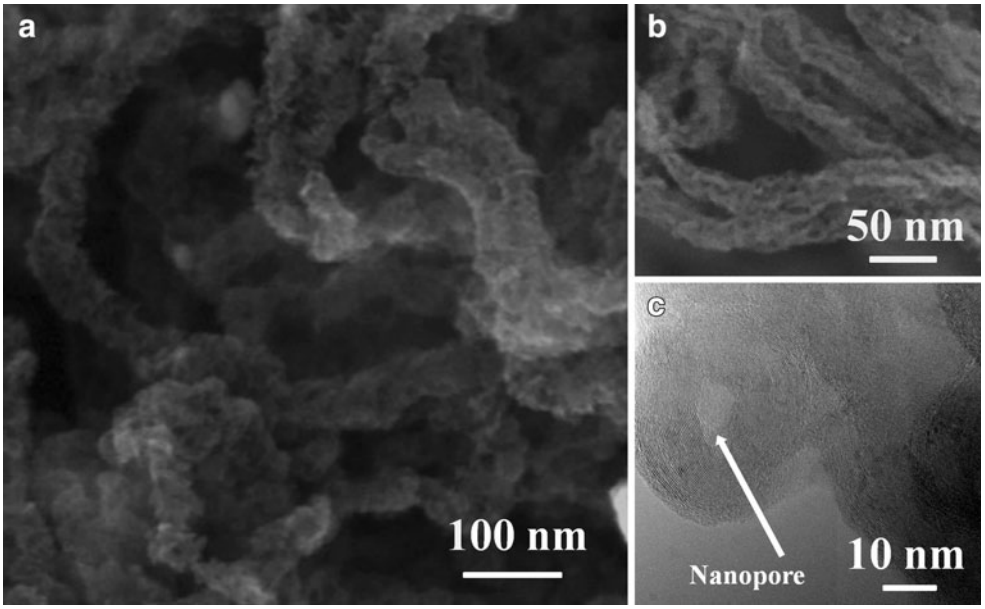


**Fig. 1** SEM images of PCNFs with **a** low and **b** high magnification. **c** TEM image of the pore structure of PCNFs

section of the film). For comparison, GOD/BMIM·$PF_6$/CHIT/GCEs, GOD/PCNFs/CHIT/GCEs, and PCNFs/BMIM·$PF_6$/CHIT/GCEs were also prepared with the same procedures described above. The sensing area of the GOD/BMIM·$PF_6$/CHIT/GCE was determined using cyclic voltammetry. This was based on the Randles–Sevčik equation [34]: $I_p = 2.69 \times 10^5 (n)^{3/2}(v)1/2A(D)^{1/2}C_o$. where $I_p$ is the peak current (A), $n$ is the number of electrons transferred, $A$ is the electrode area ($cm^2$), $D$ is the diffusion coefficient of the electro-active species ($cm^2\ s^{-1}$), $C_o$ is the bulk concentration of the same species (mol $cm^{-3}$), and $v$ is the scan rate (V $s^{-1}$). In this paper, cyclic voltammetric experiments were performed in 1.0 mM $K_3[Fe(CN)_6]$ and 0.1 M KCl solution. The sensing area of the film-modified GCE was determined as 0.095 $cm^2$.

### Assay of the GOD activity before and after the immobilization

The activity assay for free and immobilized GOD was carried out according to a modified version of Sigma Bulletin [35]. For that purpose, different concentrations of glucose solutions (2.0–20.0 mM) were prepared (in buffer). Then, they were placed in water bath, shaken for 10 min at 25 °C for pre-incubation. GOD/PCNFs/BMIM·$PF_6$/CHIT/GCE was then placed in glucose solution and the reaction was carried out for specific times. After removing the electrode, 0.5 mL of aliquots were drawn and 0.1 mL peroxidase (60 U $mL^{-1}$), 2.4 mL *o*-dianisidine (21 mM) as the reducing agent were added. The reaction was stopped with the addition of 0.5 mL sulfuric acid (2.5 M). After mixing, absorbances for blank and the solution were measured at 530 nm. For the free GOD, different concentrations of glucose solutions were prepared and pre-incubated in water bath for 10 min at 25 °C. Then 0.1 mL GOD was added and reacted for specific times. The rest of the procedure was the same as the GOD/PCNFs/BMIM·$PF_6$/CHIT/GCE case. Under the optimum conditions, the typical amount of GOD incorporated in the PCNFs/BMIM·$PF_6$/CHIT/GCE is the typical amount of GOD incorporated in the PCNFs/BMIM·$PF_6$/CHIT/GCE is 0.57 U (i.e., 6 U $cm^{-2}$ of the electrode's surface).

## Results and discussion

### Characterization of the GOD/PCNFs/BMIM·$PF_6$/CHIT composite film

UV–vis spectroscopy is a useful tool for monitoring possible changes of the absorption band in the GOD group region of the composite film. Figure 2a shows the UV–vis spectra of CHIT, PCNFs/BMIM·$PF_6$/CHIT, GOD, and GOD/PCNFs/BMIM·$PF_6$/CHIT. The UV–vis spectrum of the sample with free GOD (curve c) reveals two peaks that represent the characteristic of the oxidized form of flavin groups at about 380 and 450 nm [36]. The position and shape of the adsorption bands (378 and 454 nm) for GOD in GOD/PCNFs/BMIM·$PF_6$/CHIT composite (Fig. 2a, curve d) are almost the same as those with free GOD, suggesting that the chromophoric groups of FAD responsible for the GOD visible adsorption spectrum should be embedded in the GOD polypeptide matrix. The chromophoric groups did not come out of the pockets during the process of immobilization of GOD on PCNFs/BMIM·$PF_6$/CHIT. The spectra of free GOD and the GOD/PCNFs/

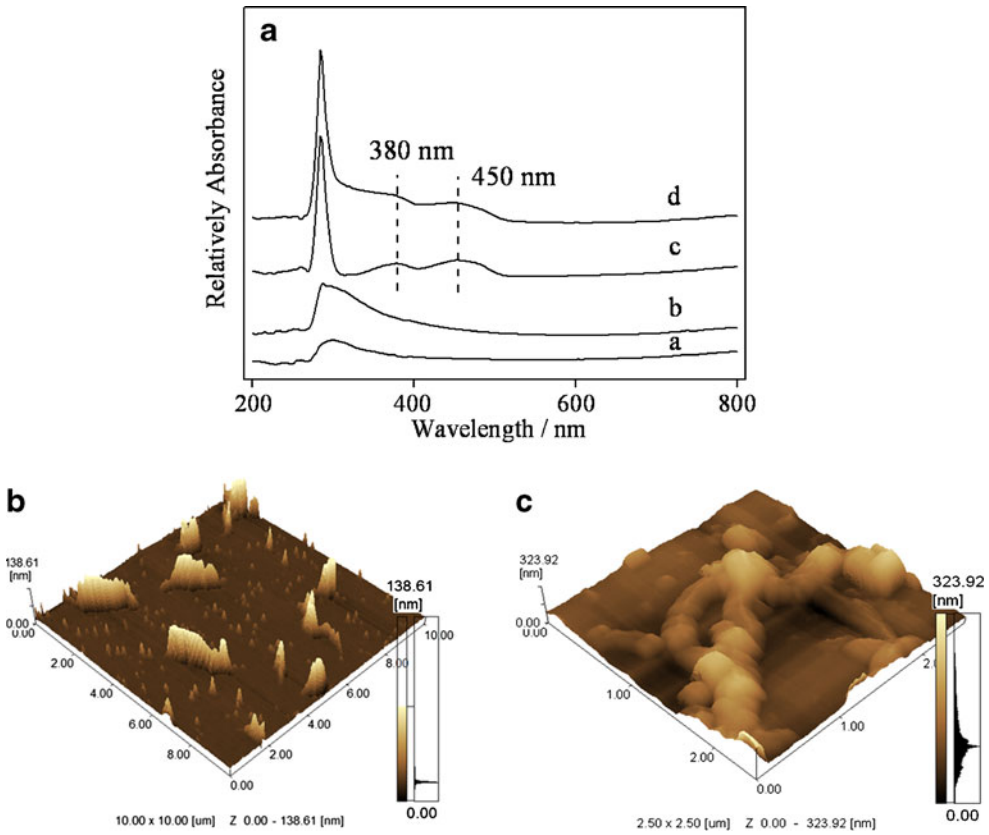


**Fig. 2** **a** UV–vis absorption spectra of (*a*) CHIT, (*b*) PCNFs/BMIM·$PF_6$/CHIT, (*c*) GOD, and (*d*) GOD/PCNFs/BMIM·$PF_6$/CHIT; AFM images of **b** PCNFs and **c** GOD-adsorbed PCNFs

BMIM·$PF_6$/CHIT at about 275 and 287 nm in both the cases are due to the e–e* transitions arising from the tryptophan and tyrosine residues on the enzyme surface [37]. Figure 2b, c present AFM images of PCNFs and GOD adsorbed onto PCNFs on the mica substrates. The distinct globular structures on the PCNFs represent GOD molecules. As shown in the AFM image (Fig. 2c), GOD molecules were aggregated on PCNFs due to the large surface-to-volume ratio and high pore structure of PCNFs.

BMIM·$PF_6$ plays a key role in the supported PCNFs/BMIM·$PF_6$/CHIT composite film-modified electrode, the homogeneous functionalization of PCNFs and the direct electron transfer of GOD [30, 38]. First, BMIM·$PF_6$ can mix well with CHIT aqueous solution to form a homogenous solution, which can be readily immobilized onto the GC electrode surface and form a stable film after it is being dried. The relatively high viscosity and the delocalized π interaction between them provided us a possibility to fabricate this specific structure. Secondly, the high conductive BMIM·$PF_6$ could also act as a supporting electrolyte itself and thus accelerate the electron transfer between the redox center of GOD and the electrode. Thirdly, the hydrophobic microenvironment of PCNFs/BMIM·$PF_6$ gel can prevent the stripping of essential water from the enzyme's polypeptide lattice which will change a protein conformation and cause loss of enzyme activity [39].

## Direct electron transfer of GOD within the PCNFs/BMIM·$PF_6$/CHIT composite film

Figure 3 shows typical cyclic voltammograms of different modified electrodes in 0.05 M pH 7.0 PBS. A pair of well-defined redox peaks of GOD was observed at the GOD/PCNFs/BMIM·$PF_6$/CHIT/GCE (Fig. 3, curve d). The formal potential $E^{\circ\prime}\left(E^{\circ\prime} = \left(E_{p,a} + E_{p,c}\right)/2\right)$ of GOD was −0.45 V (vs. SCE). Such peaks can be ascribed to the

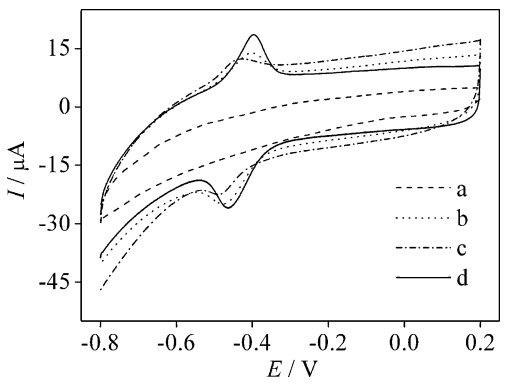


**Fig. 3** Cyclic voltammograms of (*a*) PCNFs/BMIM·$PF_6$/CHIT/GCE, (*b*) GOD/BMIM·$PF_6$/CHIT/GCE, (*c*) GOD/PCNFs/CHIT/GCE, and (*d*) GOD/PCNFs/BMIM·$PF_6$/CHIT/GCE in pH 7.0 0.05 M PBS, scan rate, 50 mV $s^{-1}$

redox reaction of the prosthetic FAD bound to GOD [8, 17, 31]. The potential difference $\Delta E_p$ between the anodic and cathodic peak potentials was about 60 mV. Such a small $\Delta E_p$ value revealed a fast and quasi-reversible electron transfer process. For comparison, the prepared electrode without GOD did not show any redox waves in the same potential range (Fig. 3, curve a). Moreover, in comparison with GOD/PCNFs/BMIM·$PF_6$/CHIT/GCE, the redox peaks observed at the GOD/BMIM·$PF_6$/CHIT/GCE and the GOD/PCNFs/CHIT/GCE (Fig. 3, curves b and c) were smaller. It can be clearly seen from the comparison that direct electron transfer between GOD molecules and GCE was enhanced at the GOD/PCNFs/BMIM·$PF_6$/CHIT composite film-modified electrode. It can therefore be concluded that the combination of BMIM·$PF_6$ with PCNFs had better performance on the facilitation of electron transfer, which may be resulted from the larger surface area, the porous framework of the PCNFs and some kind of non-covalent interactions between PCNFs and the imidazole loop of BMIM·$PF_6$. Moreover, at neutral pH GOD carries an overall negative charge and is probably immobilized onto the PCNFs/BMIM·$PF_6$ composites as a counterion.

The effect of scan rate on the voltammetric response of GOD in the composite film was investigated in 0.05 M PBS (pH 7.0) solution (Fig. 4). With scan rate ($v$) increased from 10 to 1,000 mV $s^{-1}$, the redox peak potentials of GOD remained almost unchanged and currents increased linearly, showing a surface-controlled electrode process. According to the equation $I_p = n^2F^2vA\Gamma/4RT$ [40], where $\nu$ is the scan rate, $A$ is the modified film surface area (0.095 $cm^2$), and the other symbols have their usual meanings. The surface coverage ($\Gamma$) of GOD on the electrode surface was estimated to be $7.2\times10^{-11}$ mol $cm^{-2}$ ($n$=2) from the slope of the $I_p$–$v$ curve. This value is much larger than the theoretical value ($2.86\times10^{-12}$ mol $cm^{-2}$) for the monolayer of GOD on the bare electrode surface [41], suggesting that the nanostructured PCNFs provide a large active area for enzyme immobilization.

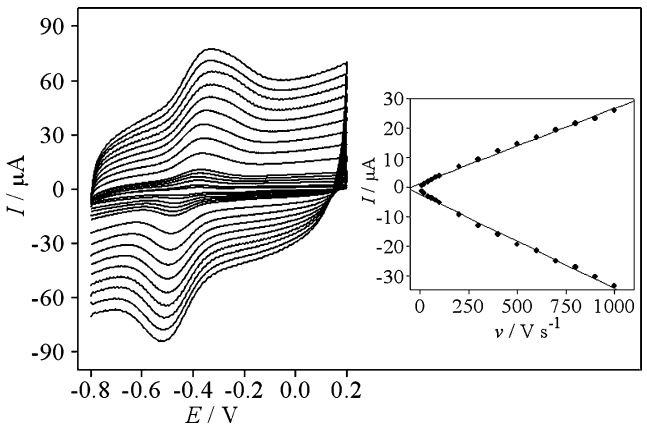


**Fig. 4** Cyclic voltammograms of the GOD/PCNFs/BMIM·$PF_6$/CHIT composite film-modified electrode in pH 7.0 0.05 M PBS solution at various scan rates (from inner to outer curve): 20, 40, 60, 80, 100, 200, 300, 400, 500, 600, 700, 800, 900, and 1,000 mV $s^{-1}$. *Inset* Plots of peak currents vs. scan rates

At higher scan rates, the plot of peak currents vs. scan rate deviated from linearity and the peak currents became proportional to the square root of the scan rates, which indicates the limitation arising from charge transfer kinetics. Based on the Laviron theory, the electron transfer rate constant $k_s$ can be calculated. The calculated value of $k_s$ was 3.4 $s^{-1}$. Herein, the larger value of $k_s$ indicates that the electron communication between the active site of GOD and electrode is not shielded by the globular protein shell of GOD in some extent and even it is further facilitated greatly. The possible reasons for an enhanced electron transfer may be ascribe to two aspects: (1) the PCNFs/BMIM·$PF_6$ composite have good electrical conductivity; (2) the PCNFs/BMIM·$PF_6$ composite film may provide a microenvironment for GOD to undergo facile electron transfer reaction, that is interactions between GOD and PCNFs/BMIM·$PF_6$ made the electron transfer process more easier between the electro-active centers of GOD and the electrode surfaces.

Compared with BMIM·$BF_4$ and EMIM·$BF_4$, the hydrophobic BMIM·$PF_6$ is less likely to absorb water from the protein. Thus, the cyclic voltammograms of GOD immobilized in PCNFs/BMIM·$PF_6$/CHIT are well defined and stable. In the hydrophilic BMIM·$BF_4$ and EMIM·$BF_4$, the couple is much smaller, and the stability is poor. The redox couple also disappears after several consecutive cycles.

## Electrocatalytic ability of the GOD/PCNFs/BMIM·$PF_6$/CHIT/GCE

The electrocatalytic ability of the GOD/PCNFs/BMIM·$PF_6$/CHIT/GCE to the reduction of $O_2$ was firstly evaluated by cyclic voltammetry. As can be seen from Fig. 5a, in an air-saturated buffer solution, the composite film-modified electrode exhibited an obvious reduction peak toward the reduction of $O_2$ at about −0.5 V (curves c and d). In contrast, at bare GCE, no reductive peak was observed in the scan range (Fig. 5a, curves a and b). It indicated that GOD immobilized in the PCNFs/BMIM·$PF_6$/CHIT composite film retained its high electrocatalytical activity towards the reduction of $O_2$. The greatly enhanced reduction activity of dissolved $O_2$ at GOD/PCNFs/BMIM·$PF_6$/CHIT composite film-based electrochemical transducers makes the composite film extremely attractive for amperometric glucose biosensors.

Upon addition of glucose to the air-saturated buffer solution, the reduction peak current decreases along with the increase of glucose concentration (Fig. 5b). The

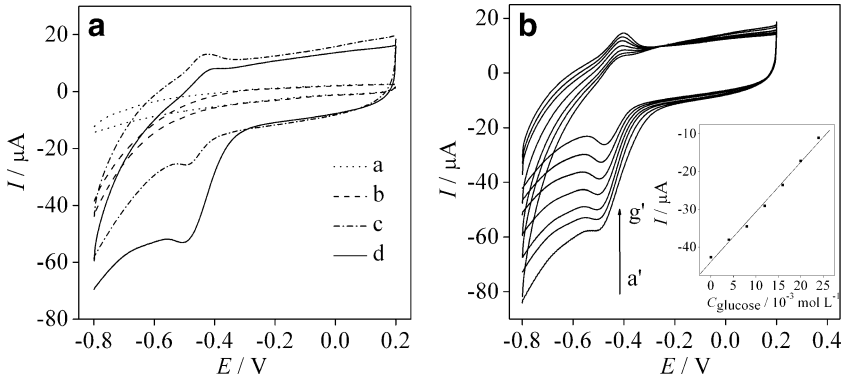


**Fig. 5** **a** Cyclic voltammograms of bare GCE and GOD/PCNFs/BMIM·$PF_6$/CHIT composite film in pH 7.0 $N_2$ saturated (*a*) and (*c*) and $O_2$-dissolved PBS solution (*b*, *d*), scan rate, 50 mV $s^{-1}$. **b** Cyclic voltammograms of the GOD/PCNFs/BMIM·$PF_6$/CHIT/GCE in pH 7.0 0.05 M PBS solution containing (*a′*) 0, (*b′*) 4.0, (*c′*) 8.0, (*d′*) 12.0, (*e′*) 16.0, (*f′*) 20.0, and (*g′*) 24.0 mM glucose at a scan rate of 50 mV $s^{-1}$. *Inset* Plot of peak current vs. glucose concentration

decrease of the reduction current of $O_2$ with the addition of glucose was employed to glucose determination. Inset of Fig. 5b shows that the peak current of the cathodic peak and the glucose concentration demonstrate a linear relationship in the range of 4.0 to 24.0 mM with a correlation coefficient of 0.996. The limit of detection was determined to be 1.3 mM with the signal-to-noise ratio of 3. The linear response obtained with the biosensor covers the clinical region for a range of 3.5–6.5 mM glucose [42], indicating that the biosensor can be possibly used in the analysis of real samples.

At higher glucose concentration, the response shows the characteristics of Michaelis–Menten kinetic mechanism. The apparent Michaelis–Menten constant ($K_m^{app}$) of the enzyme reaction at the GOD/PCNFs/BMIM·$PF_6$/CHIT/GCE was found to be 0.8 mM, which is much smaller than 6.8 mM for GOD immobilized in the CNTs/CHIT film [43] and 33 mM for native GOD in solution [44]. The high affinity of the immobilized GOD to substrate reveals the improved accessibility of enzyme-substrate and the good biocompatibility of the PCNFs/BMIM·$PF_6$/CHIT composite.

The effects of the film thickness on the performance of the biosensor were studied by cyclic voltammetry and SEM. The film thickness can be adjusted by varying the total amount of the GOD/PCNFs/BMIM·$PF_6$/CHIT mixture. Results showed that an increase in response of the GOD/PCNFs/BMIM·$PF_6$/CHIT film to glucose when the film thickness was 2.0 μm. When GOD loading is lower, the response current increases with increment of GOD loading. This indicates that the catalytic currents are controlled by the GOD activity in the composite film. However, too thick a modified film was not good for biosensor response as this will increase the diffusion barrier. Thus, the thickness of the GOD/PCNFs/BMIM·$PF_6$/CHIT film was estimated to be ca. 2.0 μm based on the optimum fabrication conditions.

## Stability and reproducibility of the biosensor

After several initial scans, the cyclic voltammogram remains nearly unchanged for 100 cycles. When the resulting film-modified electrodes were stored at 4 °C for 5 weeks, the current response is still retained, which suggested that the electrode has an excellent stability. This good stability can be attributed to the presence of large amount of pores [32] in the fiber, the electrostatic interaction of GOD and BMIM·$PF_6$, and the synergistic performance of PCNFs and RTILs which can provide a favorable microenvironment for GOD to retain its bioactivity. The fabrication reproducibility of six electrodes, made independently, shows an acceptable reproducibility with the RSD of 4.6%.

## Application to glucose determination

The determination of glucose in human plasma was performed by using the glucose biosensor utilizing standard addition

**Table 1** Determination of glucose in human plasma samples by the proposed biosensor

| Sample no. | Found (mM) | Added (mM) | Found (mM) | Recovery/% |
|---|---|---|---|---|
| 1 | 4.65 | 2.0 | 6.45 | 95.7 |
| 2 | 5.05 | 2.0 | 7.15 | 101.2 |
| 3 | 4.70 | 2.0 | 6.85 | 103.2 |

The average value of three measurements

method. After the current response was determined in 10.0 mL of 0.05 M PBS (pH 7.0) solution containing sample of 1.0 mL, 20 μL of 1.0 M glucose was added to the system for standard addition determination. The measurement results are listed in Table 1. The average measurement result is found to be 4.8 mM. The recoveries for the determination of glucose are between 95.7% and 103.2% for three times. The interference effects were also tested by recording SWV responses of 0.1 mM glucose in the presence of different concentrations of uric acid or ascorbic acid. Results showed that no obvious current changes occurred, even with the concentration of uric acid or ascorbic acid up to 0.1 or 0.2 mM, respectively. This is enough to limit the interference effects for real sample analysis.

## Conclusions

In the present work, the direct electrochemistry of GOD immobilized in the PCNFs/BMIM·$PF_6$/CHIT composite film was achieved. PCNFs were covered with high electric conductive RTILs, which encapsulated in pores to facilitate the direct electron transfer of GOD. The composite film provided a unique microenvironment for the successful immobilization and electron transfer of GOD without the assistance of any electron mediator. The combination of the PCNFs, RTIL, and CHIT not only offers new design of stable enzymatic biosensors based on direct electrochemistry of the redox proteins but also for integration of the electrode into biofuel cells.

**Acknowledgments** The authors appreciate the financial support from the National Natural Science Foundation of China (no. 20875076), the Science Foundation of Northwest University (no. 09NW02), the Education Department of Shaanxi Province, China (no. 2010JK877), and the NWU Doctorate Dissertation of Excellence Funds (no. 08YYB06).

## References

1. Brajter-Toth A, Chambers JQ (2002) Electroanalytical methods for biological materials. Marcel Dekker, New York
2. Gooding JJ, Wibowo R, Liu, Yang JW, Losic D, Orbons S, Mearns FJ, Shapter JG, Hibbert DB (2003) J Am Chem Soc 125:9006–9007
3. Wang J (2008) Chem Rev 108:814–825
4. Guascito MR, Chirizzi D, Malitesta C, Mazzotta E (2011) Analyst 136:164–173
5. Scheller F, Schubert F (1992) Physicochemical, biochemical and technological fundamentals of biosensors. Elsevier, New York, pp 24–25
6. Liu SQ, Ju HX (2005) Biosens Bioelectron 19:177–183
7. Zhao G, Xu JJ, Chen HY (2006) Electrochem Commun 8:148–154
8. Salimi A, Sharifi E, Noorbakhsh A, Soltanian S (2007) Biosens Bioelectron 22:3146–3153
9. Sheng QL, Luo K, Li L, Zheng JB (2009) Bioelectrochemistry 74:246–253
10. Tang H, Chen JH, Yao SZ, Nie LH, Deng GH, Kuang YF (2004) Anal Biochem 331:89–97
11. Shan D, Zhang J, Xue HG, Ding SN, Cosnier S (2010) Biosens Bioelectron 25:1427–1433
12. Zhang Q, Wu SY, Zhang L, Lu J, Verproot F, Liu Y, Xing ZQ, Li JH, Song XM (2011) Biosens Bioelectron 26:2632–2637
13. Wang K, Liu Q, Guan QM, Wu J, Li HN, Yan JJ (2011) Biosens Bioelectron 26:2252–2257
14. Csöregi E, Schmidtke DW, Heller A (1995) Anal Chem 67:1240–1244
15. Yarnitzky C, Caruana AM, Schmidtke DW, Heller A (1998) J Phys Chem B 102:10057–10061
16. Mano N, Yoo JE, Tarver J, Loo YL, Heller A (2007) J Am Chem Soc 129:7006–7007
17. Xiao Y, Patolsky F, Katz E, Hainfeld JF, Willner I (2003) Science 299:1877–1881
18. Riklin A, Katz E, Willner I, Stocker A, Bückmann AF (1995) Nature 376:672–675
19. Lee D, Lee J, Kim J, Kim J, Na HB, Kim B, Shin CH, Kwak JH, Dohnalkova A, Grate JW, Hyeon T, Kim HS (2005) Adv Mater 17:2828–2833
20. Javey A, Guo J, Wang Q, Lundstrom M, Dai H (2003) Nature 424:654–657
21. Arai S, Endo M (2003) Electrochem Commun 5:797–799
22. Lu XB, Zhou JH, Lu W, Liu Q, Li JH (2008) Biosens Bioelectron 23:1236–1243
23. Chae WS, An MJ, Lee SW, Son MS, Yoo KH, Kim YR (2006) J Phys Chem B 110:6447–6450
24. Wu LN, Zhang XJ, Ju HX (2007) Biosens Bioelectron 23:479–484
25. Wu LN, Zhang XJ, Ju HX (2007) Anal Chem 79:453–458
26. Hao C, Ding L, Zhang J, Ju HX (2007) Anal Chem 79:4442–4447
27. Li JH, Shen YF, Zhang YJ, Liu Y (2005) Chem Commun 3:360–362
28. Lee JK, Kim MJJ (2002) Org Chem 67:6845–6847
29. Li JW, Fan C, Xiao F, Yan R, Fan SS, Zhao FQ, Zeng BZ (2007) Electrochim Acta 52:6178–6185
30. Liu Y, Huang LJ, Dong SJ (2007) Biosens Bioelectron 23:35–41
31. Zhang YJ, Shen YF, Han DX, Wang ZJ, Song JX, Li F, Niu L (2007) Biosens Bioelectron 23:438–443
32. Huang CW, Chiu SC, Lin WH, Li YY (2008) J Phys Chem C 112:926–931
33. Davis LH, Gordon CM, Hilgers C, Wasserscheid P, Welton T (2003) Ionic Liquid in Synthesis (Eds: Wasserscheid P, Welton T) Wiley, New York, Chapter 3
34. Gooding JJ, Praig VG, Hall EAH (1998) Anal Chem 70:2396–2402
35. The enzymatic colorimetric determination of glucose (1983) Sigma Technical Bulletin No. 510, Sigma Chemical Co., St Louis USA
36. Yang WW, Wang JX, Zhao S, Sun YY, Sun CQ (2006) Electrochem Commun 8:665–672
37. Stoscheck CM (1990) Methods Enzymol 182:50–68
38. Zhang YJ, Shen YF, Li JH, Niu L, Dong SJ, Ivaska A (2005) Langmuir 21:4797–4800
39. Wang SF, Chen T, Zhang ZL, Shen XC, Lu ZX, Pang DW, Wong KY (2005) Langmuir 21:9260–9266
40. Laviron E (1979) J Electroanal Chem 100:263–270
41. Xu JZ, Zhu JJ, Wu Q, Hu Z, Chen HY (2003) Electroanalysis 15:219–224
42. Heider GH, Sasso SV, Huang KM, Yacynych AM, Wieck HJ (1990) Anal Chem 62:1106–1110
43. Zhou QM, Xie QJ, Fu YC, Su ZH, Jia XE, Yao SZ (2007) J Phys Chem B 111:11276–11284
44. Yokogama K, Kayanuma Y (1998) Anal Chem 70:3368–3376